AIAA JOURNAL
Vol. 32, No. 6, June 1994

# Transverse Shear Stresses and Their Sensitivity Coefficients in Multilayered Composite Panels

Ahmed K. Noor,* Yong H. Kim,† and Jeanne M. Peters‡
*University of Virginia, NASA Langley Research Center, Hampton, Virginia 23681*

**A computational procedure is presented for the accurate determination of transverse shear stresses and their sensitivity coefficients in flat multilayered composite panels subjected to mechanical and thermal loads. The sensitivity coefficients measure the sensitivity of the transverse shear stresses to variations in the different lamination and material parameters of the panel. The panel is discretized by using either a three-field mixed finite element model based on a two-dimensional first-order shear deformation plate theory or a two-field degenerate solid element with each of the displacement components having a linear variation throughout the thickness of the laminate. The evaluation of transverse shear stresses can be conveniently divided into two phases. The first phase consists of using a superconvergent recovery technique for evaluating the in-plane stresses in the different layers. In the second phase, the transverse shear stresses are evaluated by using piecewise integration, in the thickness direction, of the three-dimensional equilibrium equations. The same procedure is used for evaluating the sensitivity coefficients of the transverse shear stresses. The effectiveness of the computational procedure is demonstrated by means of numerical examples of multilayered cross-ply panels subjected to transverse loading, uniform temperature change, and uniform temperature gradient through the thickness of the panel. In each case the standard of comparison is taken to be the exact solution of the three-dimensional thermoelasticity equations of the panel.**

## Nomenclature

$[A], [B], [D], [A_s]$ = matrices of the extensional, coupling, bending, and transverse shear stiffnesses
$a_{3\alpha\beta 3}$ = three-dimensional transverse shear compliance coefficients
$[\bar{B}]$ = strain-displacement matrix
$[C]$, $[\bar{C}]^{(k)}$ = effective stiffness matrix of the panel and reduced material stiffness matrix of the $k$th layer (based on neglecting the normal stress component $\sigma_{33}$)
$c_{\beta\gamma\rho\delta}$, $\bar{c}_{\beta\gamma\rho\delta}$ = elastic and reduced stiffnesses of the material, respectively
$E_L, E_T$ = elastic moduli of the individual layers in the direction of fibers and normal to it, respectively
$\{E\}, \{\bar{E}\}$ = vectors of total strain and average mechanical strain through the thickness, respectively
$G_{LT}, G_{TT}$ = shear moduli of the individual layers in the plane of fibers and normal to it, respectively
$\{H\}$ = vector of stress resultant parameters
$\{H_T\}, \{\bar{H}_T\}$ = vectors of normalized thermal forces
$h$ = total thickness of the panel
$h_k, h_{k-1}$ = distances from the top and bottom surfaces of the $k$th layer to the middle surface; see Fig. 1
$[K]$ = global structure matrix; see Eq. (1)
$[K], [\bar{K}]$ = generalized stiffness matrices; see Appendix B
$L$ = side length of the panel
$M_1, M_2, M_{12}$ = bending stress resultants
$NL$ = total number of layers in the panel
$N_1, N_2, N_{12}$ = in-plane (extensional) stress resultants
$\bar{N}_{i'}$, $\bar{N}_{j'}$ = shape functions used in approximating each of the strain components and stress resultants
$\{N\}, \{M\}$ = vectors of in-plane and bending stress resultants; see Eqs. (A1)
$\{N_T\}, \{M_T\}$ = vectors of thermal forces and moments in the panel; see Eqs. (A1)
$\{P\}$ = vector of nodal mechanical forces
$Q_1, Q_2$ = transverse shear stress resultants
$\{Q\}$ = vector of transverse shear stress resultants
$\{Q^{(1)}\}, \{Q^{(2)}\}$ = vectors of normalized mechanical and thermal loads
$[\bar{Q}]^{(k)}, [\bar{Q}_s]^{(k)}$ = matrices of the extensional and transverse shear stiffnesses of the $k$th layer of the panel (referred to $x_1, x_2, x_3$ coordinate system)
$q_1, q_2$ = mechanical and thermal loading parameters; see Eq. (1)
$[R]$ = matrix of products of shape functions; see Appendix B
$[R_1]$ = matrix of shape functions used in approximating the average mechanical strains (through the thickness)
$[S], [S_1]$ = strain-displacement matrices; see Appendix B
$T$ = temperature change
$T_0, T_1$ = amplitudes of uniform temperature change and uniform temperature gradient through the thickness, respectively
$U$ = total strain energy density for the panel; see Eq. (D5)
$u_1, u_2, w$ = displacement components in the coordinate directions; see Fig. 1
$\{X\}$ = vector of generalized nodal displacements
$x_1, x_2, x_3$ = Cartesian coordinate system ($x_3$ normal to the middle plane of the panel)
$\{Z\}$ = response vector of the panel
$\alpha_L, \alpha_T$ = coefficients of thermal expansion of the individual layers in the direction of fibers and normal to it, respectively
$\{\alpha\}^{(k)}$ = vector of coefficients of thermal expansion of the $k$th layer of the panel (referred to the $x_1, x_2, x_3$ coordinate system)
$\alpha_{\beta\gamma}$ = coefficients of thermal expansion
$\{\gamma\}$ = vector of transverse shear strain components of the panel; see Eqs. (A1)
$\varepsilon_{33}$ = transverse normal strain component

Received Aug. 14, 1993; revision received Nov. 10, 1993; accepted for publication Nov. 16, 1993. 

*Ferman W. Perry Professor of Aerospace Structures and Applied Mechanics, and Director, Center for Computational Structures Technology. Fellow AIAA.
†Research Associate, Center for Computational Structures Technology.
‡Senior Programmer Analyst, Center for Computational Structures Technology.

$\{\varepsilon\}$ = vector of extensional strain components of the panel; see Eqs. (A1)
$\varepsilon_{\beta\gamma}$, $\varepsilon^0_{\beta\gamma}$ = in-plane strain components at any point in the panel and at the middle plane, respectively
$\{\varepsilon\}^{(e)}_{\text{mech}}$, $\{\bar{\varepsilon}\}^{(e)}_{\text{mech}}$ = actual mechanical strain and average mechanical strain (through the thickness) for individual finite elements; see Eqs. (C1) and (C3)
$\{\bar{\varepsilon}\}^{(e)}_{\text{tot}}$ = total strain vector for individual elements; see Eqs. (C2)
$2\varepsilon_{\beta 3}$ = transverse shear strain component
$\{\kappa\}$ = vector of bending strain components of the panel; see Eqs. (A1)
$\kappa^0_{\beta\gamma}$ = curvature changes and twist of the panel
$\lambda$ = material parameter of the panel
$\upsilon_{LT}$ = major Poisson's ratio of the individual layers
$\xi_1$, $\xi_2$ = dimensionless coordinates ($\xi_\beta = x_\beta/L$; $\beta = 1, 2$)
$\sigma_{\beta\gamma}$, $\sigma_{3\beta}$ = in-plane and transverse shear stress components, respectively
$\Omega^{(e)}$ = element domain

*Subscripts*

$i', j'$ = 1 to the number of shape functions used in approximating each of the strain components (or stress resultants)
$j$ = 1 to the number of shape functions used in approximating each of the displacement components
$k$ = $k$th layer
$L$ = direction of fibers
$T$ = transverse direction
$\beta,\gamma,\rho,\delta$ = 1, 2

*Superscripts*

$k$ = $k$th layer
$t$ = matrix transposition

## I. Introduction

IT has long been recognized that the first-order shear deformation theory, based on linear displacement distribution through the entire laminate, is not adequate for the accurate determination of transverse shear stresses. Most of the advanced composites in use to date have a low ratio of the transverse shear modulus to the in-plane modulus, and therefore, the interlaminar shear stresses are important in predicting the onset of some of the damage mechanisms in multilayered composite panels. Also, since it is difficult to measure the transverse shear properties of composites, a study of the sensitivity of interlaminar stresses to variations in material properties is desirable. Only a few studies have addressed this issue.

Various techniques have been proposed for the accurate determination of transverse shear stresses in laminated composites. These include using 1) three-dimensional, or quasi-three-dimensional, finite elements (see, for example, Refs. 1–4); 2) two-dimensional finite elements based on higher-order shear deformation theories, with either nonlinear or piecewise linear approximations for the displacements in the thickness direction (see, for example, Ref. 5); and 3) two-dimensional finite elements based on the classical or first-order shear deformation theory (with linear displacement approximation through the thickness of the entire laminate) and integration in the thickness direction, of the three-dimensional equilibrium equations.[6,7]

None of the cited references considered transverse stresses in thermally loaded laminates, or their sensitivity coefficients. The sensitivity coefficients measure the sensitivity of the transverse shear stresses to variations in the different lamination and material parameters of the panel. The present study focuses on transverse shear stresses and their sensitivity coefficients in thermomechanically loaded laminates. Specifically, the objective of this paper is to present a computational procedure for the accurate determination of the transverse shear stresses and their sensitivity coefficients in multilayered composite panels subjected to mechanical and thermal loads.

Experience with most of the three-dimensional finite elements, and two-dimensional finite elements based on higher-order shear deformation theories, has shown that unless the three-dimensional equilibrium equations are used in evaluating the thickness distribution of the transverse shear stresses, the resulting transverse stresses are inaccurate (see, for example, Refs. 8–12). Since the finite element models based on the first-order shear deformation theory are considerably less expensive than those based on three-dimensional and higher-order two-dimensional theories, they have been adopted in the present study. The effectiveness of the computational procedure is demonstrated by means of numerical examples of multilayered cross-ply panels.

## II. Finite Element Formulation

The panel is discretized by using either 1) a two-dimensional three-field mixed finite element model, or 2) a two-field degenerate solid element with each of the displacement components having a linear variation throughout the thickness of the laminate.

The analytical formulation for the first finite element model is based on a first-order shear deformation plate theory with the effects of average transverse shear deformation through the thickness and laminated anisotropic material behavior included. A linear Duhamel-Neumann-type, constitutive model is used, and the material properties are assumed to be independent of temperature. The thermoelastic constitutive model is used and the material properties are assumed to be independent of temperature. The thermoelastic constitutive relations used in the present study are given in Appendix A. The fundamental unknowns consist of the total strain components, the stress resultants, and the generalized displacements. The analytical formulation for the second model is based on a linear quasi-three-dimensional thermoelasticity theory, with the transverse normal stresses neglected, but the transverse normal strains included. The fundamental unknowns consist of the average mechanical strains through the thickness and the displacement components. In both models the strain components and stress resultants are allowed to be discontinuous at interelement boundaries. Henceforth, the three-field and two-field models will be referred to as models 1 and 2, respectively. The sign convention for generalized displacements and stress resultants is shown in Fig. 1. The external loading consists of transverse static loading $p$, temperature change that is uniform in the thickness direction (independent of $x_3$), and uniform temperature gradient in the thickness direction (linear in $x_3$).

### A. Governing Finite Element Equations

The governing finite element equations describing the linear static response of the panel can be written in the following compact form:

$$[K]\{Z\} - q_1\{Q^{(1)}\} - q_2\{Q^{(2)}\} = 0 \tag{1}$$

The form of the arrays $[K]$, $\{Q^{(1)}\}$ and $\{Q^{(2)}\}$ for the two models used in the present study is described in Appendices B and C.

### B. Sensitivity Coefficients

The sensitivity coefficients for the panel response are obtained by differentiating Eqs. (1) with respect to the lamination and material parameters of the panel. The resulting equations for the first-order and second-order sensitivity coefficients can be written in the following compact form:

$$[K]\left\{\frac{\partial Z}{\partial\lambda}\right\} = -\left[\frac{\partial K}{\partial\lambda}\right]\{Z\} - q_2\left\{\frac{\partial Q^{(2)}}{\partial\lambda}\right\} \tag{2}$$

$$[K]\left\{\frac{\partial^2 Z}{\partial\lambda^2}\right\} = -2\left[\frac{\partial K}{\partial\lambda}\right]\left\{\frac{\partial Z}{\partial\lambda}\right\} - \left[\frac{\partial^2 K}{\partial\lambda^2}\right]\{Z\} - q_2\left\{\frac{\partial^2 Q^{(2)}}{\partial\lambda^2}\right\} \tag{3}$$

In Eqs. (2) and (3) $\lambda$ refers to a typical lamination or material parameter of the panel, and the mechanical loading is assumed to be independent of $\lambda$. Note that the evaluation of $[\partial \boldsymbol{K}/\partial\lambda]$, $[\partial^2 \boldsymbol{K}/\partial\lambda^2]$, $\{\partial Q^{(2)}/\partial\lambda\}$, and $\{\partial^2 Q^{(2)}/\partial\lambda^2\}$ requires differentiating the thermoelastic equations given in Appendix A and the arrays given in Appendices B and C with respect to $\lambda$.

## III. Computational Procedure

The evaluation of the thickness distribution of the transverse shear stresses can be conveniently divided into two phases. The first phase consists of solving Eqs. (1) and then using a superconvergent recovery technique for evaluating the in-plane stresses in the different layers. For optimum accuracy with a given rectangular finite element model, the in-plane stresses are calculated at the numerical quadrature points. In the second phase the thickness distributions of the transverse shear stresses are evaluated by using piecewise integration, in the thickness direction, of the three-dimensional equilibrium equations. For optimum accuracy with rectangular elements the transverse shear stresses are evaluated at the numerical quadrature points and then interpolated to the center of the element (this is because the three-dimensional equilibrium equations are only satisfied in an integral sense for each individual element, and not pointwise). The procedure for evaluating the transverse shear stresses is outlined in Appendix D.

The aforementioned procedure is also used for evaluating the thickness distributions of the sensitivity coefficients of the transverse shear stresses, using the corresponding sensitivity coefficients for the in-plane stresses in the different layers.

## IV. Numerical Studies

To assess the effectiveness of the foregoing computational procedure for evaluating the transverse shear stresses and their sensitivity coefficients, several multilayered composite panels were analyzed. The panels were subjected to various mechanical and thermal loads. For each problem considered, the transverse shear stresses, total strain energy density, and their sensitivity coefficients (first-order and second-order derivatives with respect to various material and lamination parameters) obtained by the foregoing procedure, in conjunction with two-dimensional finite element models (models 1 and 2), were compared with those obtained by the *exact* analytic solution of the three-dimensional thermoelastic equations of the panel, as well as with the predictions of an 18-node three-dimensional finite element model.[13] The exact three-dimensional thermoelasticity solutions were obtained by using the procedure described in Refs. 14 and 15, and are used as the standard for comparison. The three-dimensional finite element model was used to model each layer of the laminate. The composite shear correction factors for model 1 were taken to be 5/6. A typical problem set is considered herein, namely, that of the linear thermoelastic static response of square, 10-layer cross-ply laminates with $L = 1$, and $h/L = 0.05$ and 0.1. The fiber orientation of the laminates is $[0/90/0/90/0]_s$. The panels are subjected to either 1) transverse loading $p = p_0 \sin \pi\xi_1 \sin \pi\xi_2$, with half the loading applied at each of the top and bottom surfaces, 2) uniform temperature change through the thickness $T = T_0 \sin \pi\xi_1 \sin \pi\xi_2$, or 3) uniform temperature gradient through the thickness $T = x_3 T_1 \sin \pi\xi_1 \sin \pi\xi_2$, where $\xi_\alpha = x_\alpha/L$ $-(\alpha = 1, 2)$, and $p_0$, $T_0$, and $T_1$ are constants. Henceforth, the three cases will be referred to as the $p_0$, $T_0$, and $T_1$ cases, respectively. The material properties of the individual layers are taken to be those typical of high-modulus fibrous composites, namely, $E_L/E_T = 15$, $G_{LT}/E_T = 0.5$, $G_{TT}/E_T = 0.3378$, $\nu_{LT} = 0.3$, $\nu_{TT} = 0.48$, $\alpha_L = 0.139 \times 10^{-6}$, $\alpha_T = 9 \times 10^{-6}$, $p_0 = 1$, $T_0 = 1$, and $T_1 = 1$.

To test the accuracy of the thickness distributions of the transverse shear stresses and the total strain energy density, predicted by the two-dimensional and three-dimensional finite element models, successive refinement was made in each of the $x_1$ and $x_2$ directions until convergence was achieved. Typical results are presented in Figs. 2–5 for the response quantities and in Figs. 6–8 for

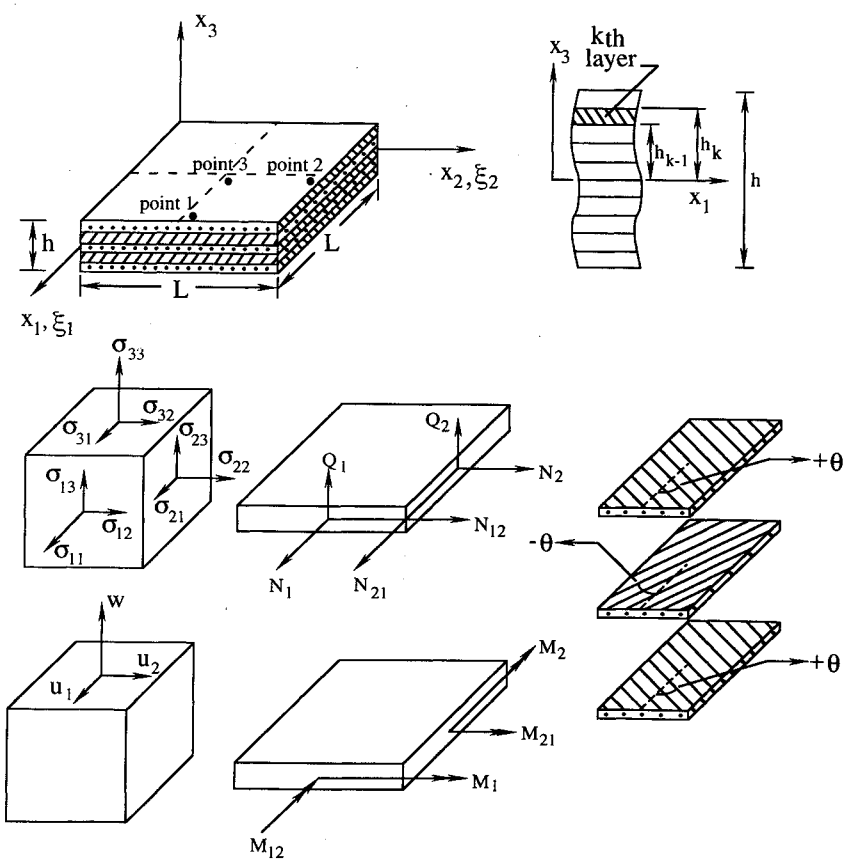


**Fig. 1 Composite panels and sign convention for displacements, stresses, and stress resultants.**

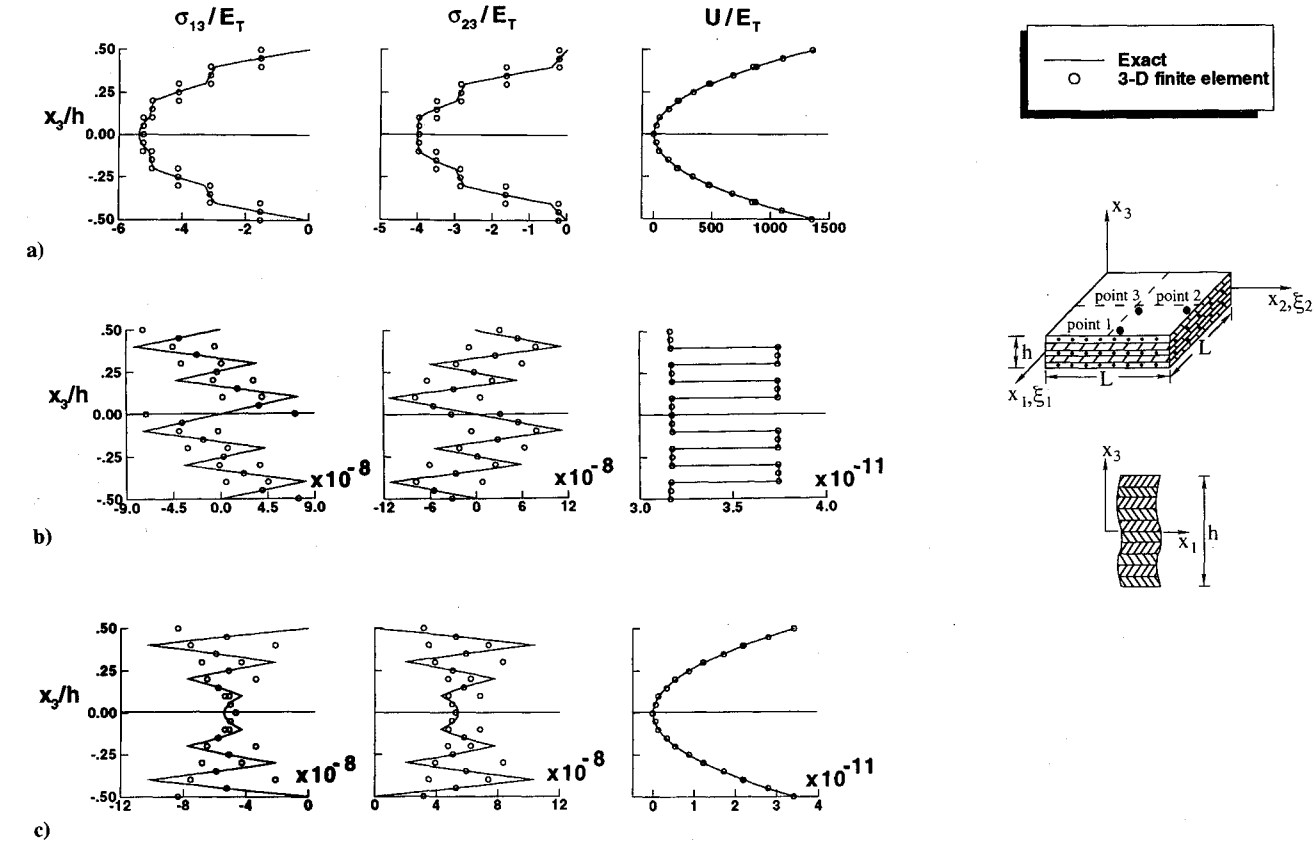


Fig. 2 Through-the-thickness distributions of transverse shear stresses $\sigma_{13}$ and $\sigma_{23}$ and strain energy density $U$ obtained by three-dimensional finite element model; 10-layer cross-ply composite panel with $h/L = 0.05$: a) static loading $p = p_0 \sin \pi\xi_1 \sin \pi\xi_2$, b) temperature change $T = T_0 \sin \pi\xi_1 \sin \pi\xi_2$, and c) temperature gradient $T = x_3 T_1 \sin \pi\xi_1 \sin \pi\xi_2$.

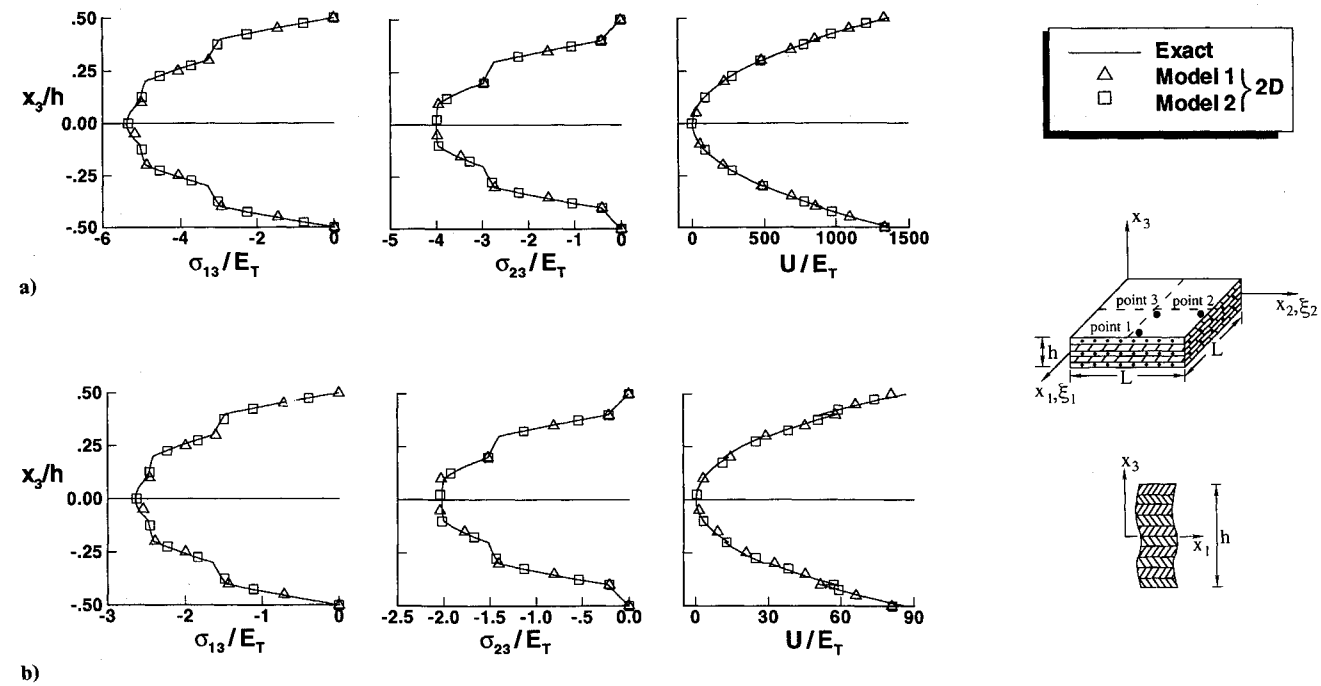


Fig. 3 Through-the-thickness distributions of transverse shear stresses $\sigma_{13}$ at point 1, $\sigma_{23}$ at point 2, and strain energy density $U$ at point 3, obtained by proposed computational procedure; 10-layer cross-ply composite panel subjected to static loading $p = p_0 \sin \pi\xi_1 \sin \pi\xi_2$: a) $h/L = 0.05$ and b) $h/L = 0.10$.

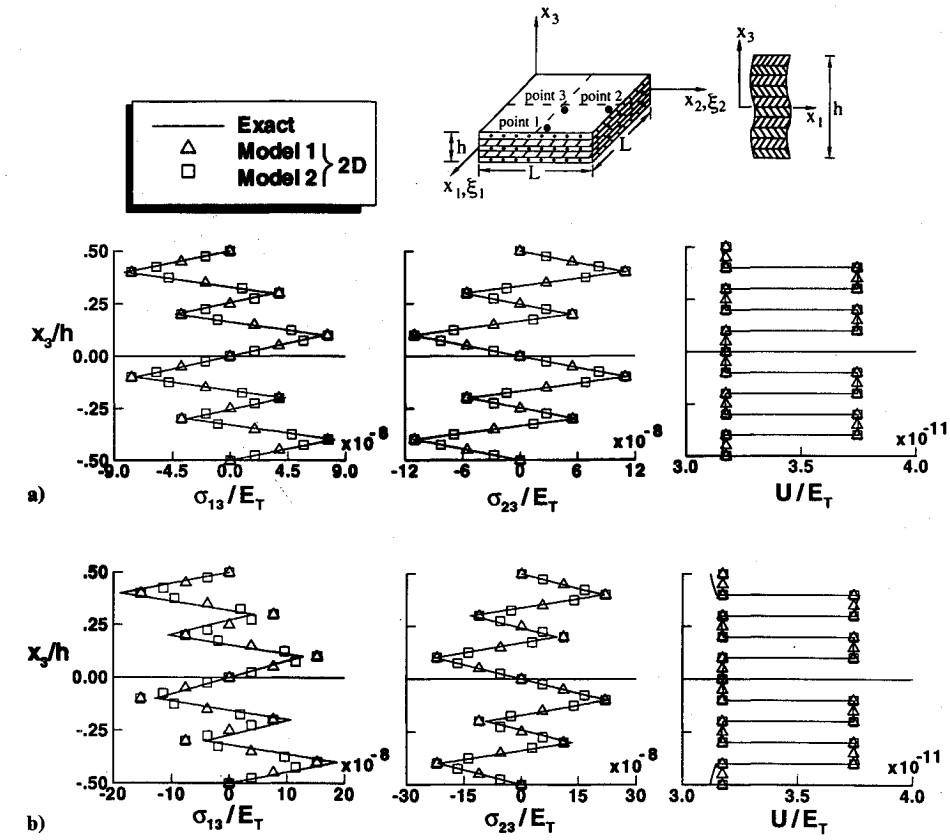


Fig. 4 Through-the-thickness distributions of transverse shear stresses $\sigma_{13}$ at point 1, $\sigma_{23}$ at point 2, and strain energy density $U$ at point 3, obtained by proposed computational procedure; 10-layer cross-ply composite panel subjected to temperature gradient $T = T_0 \sin \pi\xi_1 \sin \pi\xi_2$: a) $h/L = 0.05$ and b) $h/L = 0.10$.

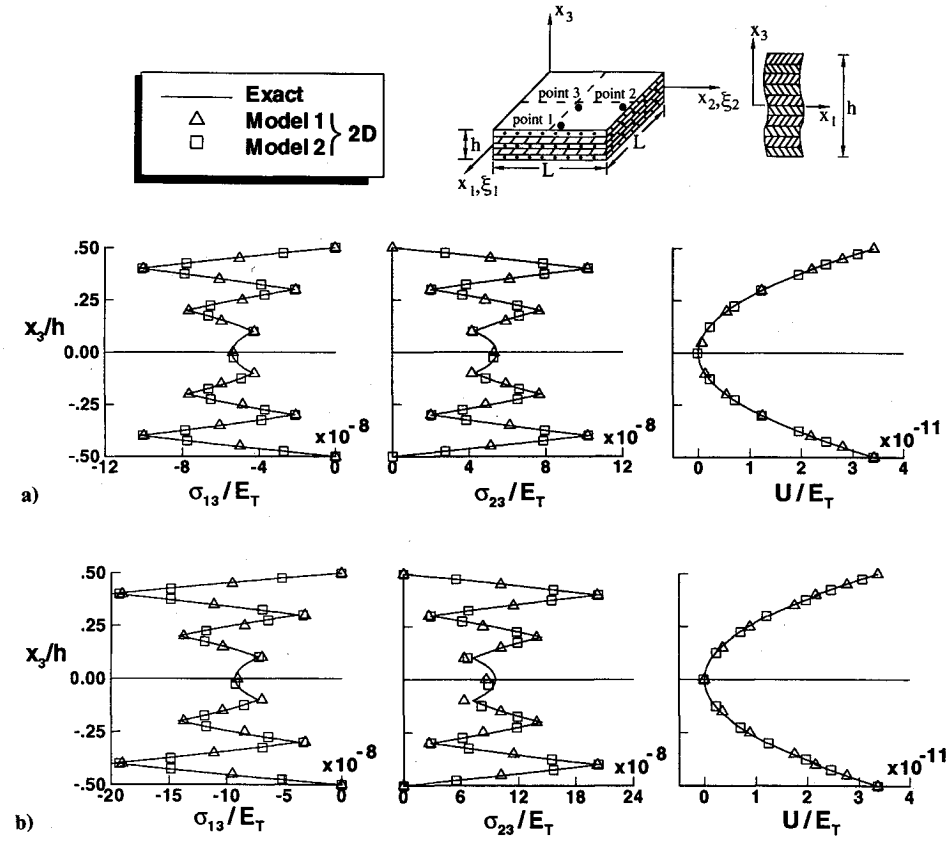


Fig. 5 Through-the-thickness distributions of transverse shear stresses $\sigma_{13}$ at point 1, $\sigma_{23}$ at point 2, and strain energy density $U$ at point 3, obtained by three-dimensional model; 10-layer cross-ply composite panel subjected to temperature gradient $T = x_3 T_1 \sin \pi\xi_1 \sin \pi\xi_2$: a) $h/L = 0.05$ and b) $h/L = 0.10$.

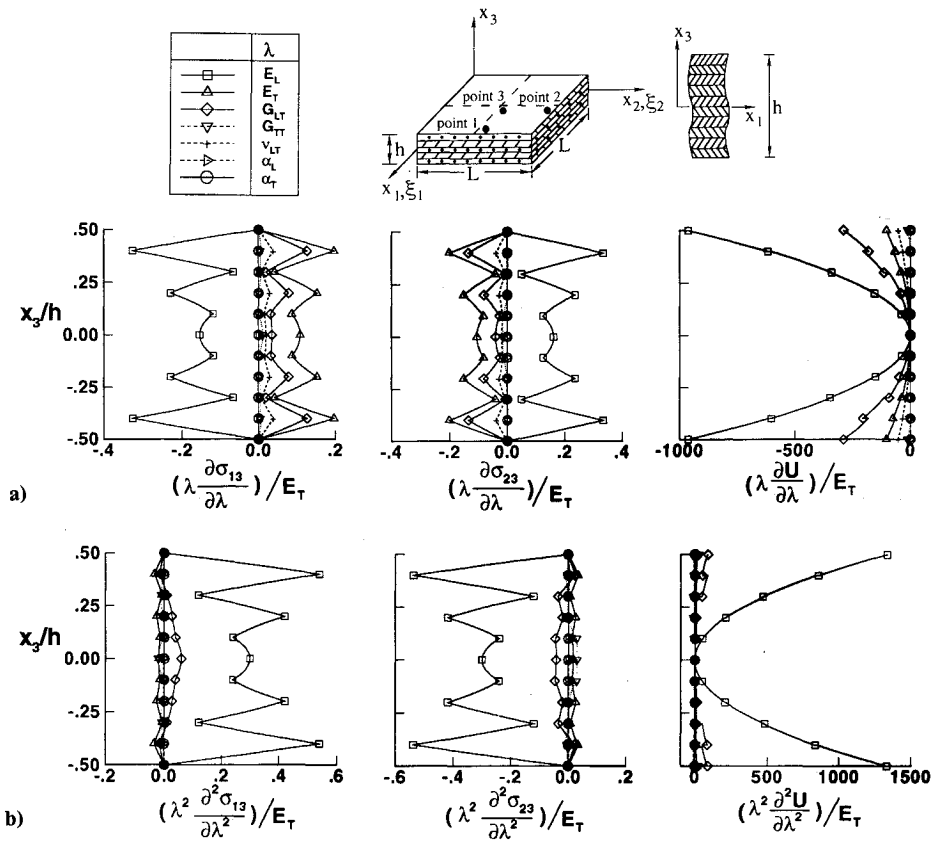


**Fig. 6** Through-the-thickness distributions of first-order and second-order sensitivity coefficients of transverse shear stresses $\sigma_{13}$ at point 1, $\sigma_{23}$ at point 2, and strain energy density $U$ at point 3 obtained by the proposed computational procedure; 10-layer cross-ply composite panel subjected to static loading $p = p_0 \sin \pi\xi_1 \sin \pi\xi_2$: a) first-order sensitivity coefficients and b) second-order sensitivity coefficients.

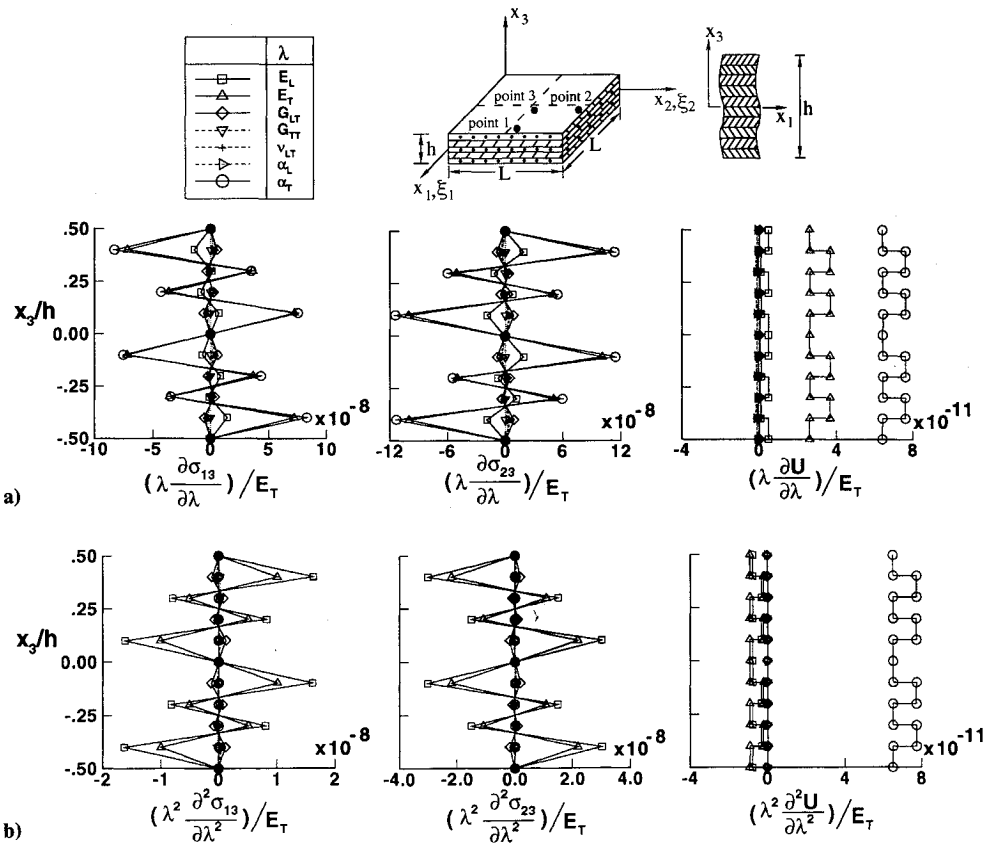


**Fig. 7** Through-the-thickness distributions of first-order and second-order sensitivity coefficients of transverse shear stresses $\sigma_{13}$ at point 1, $\sigma_{23}$ at point 2, and strain energy density $U$ at point 3 obtained by the proposed computational procedure; 10-layer cross-ply composite panel subjected to temperature change $T = T_0 \sin \pi\xi_1 \sin \pi\xi_2$: a) first-order sensitivity coefficients and b) second-order sensitivity coefficients.

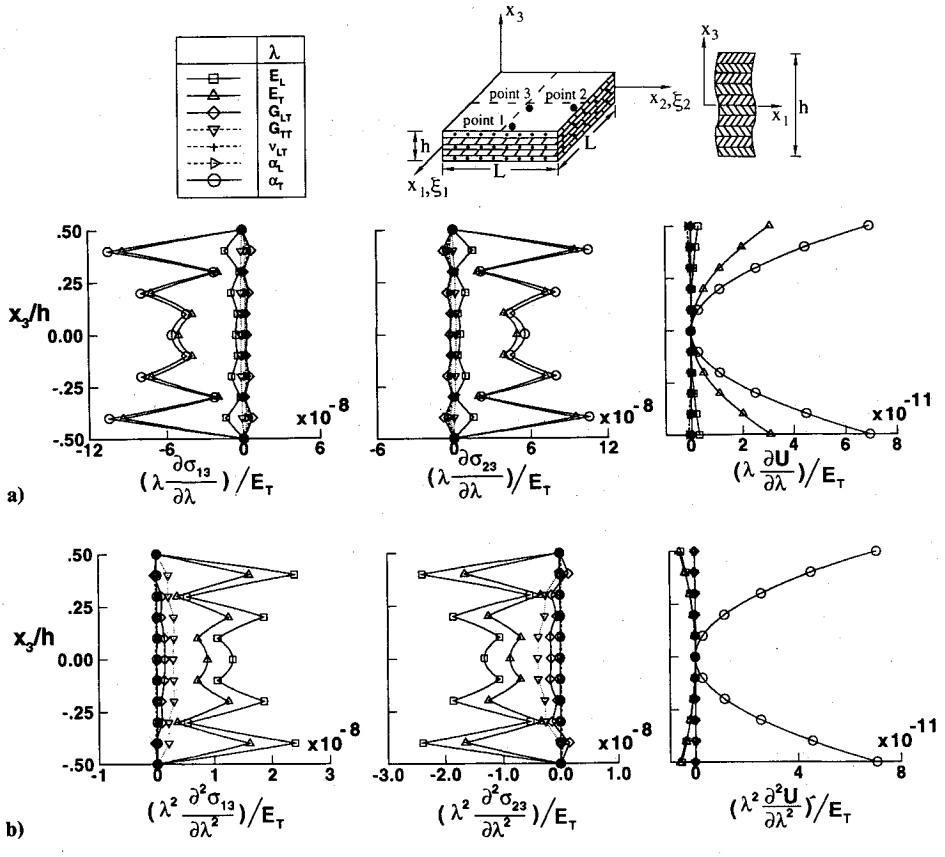


Fig. 8 Through-the-thickness distributions of first-order and second-order sensitivity coefficients of transverse shear stresses $\sigma_{13}$ at point 1, $\sigma_{23}$ at point 2, and strain energy density $U$ at point 3 obtained by the proposed computational procedure; 10-layer cross-ply composite panel subjected to temperature gradient $T = x_3 T_1 \sin \pi\xi_1 \sin \pi\xi_2$: a) first-order sensitivity coefficients and b) second-order sensitivity coefficients.

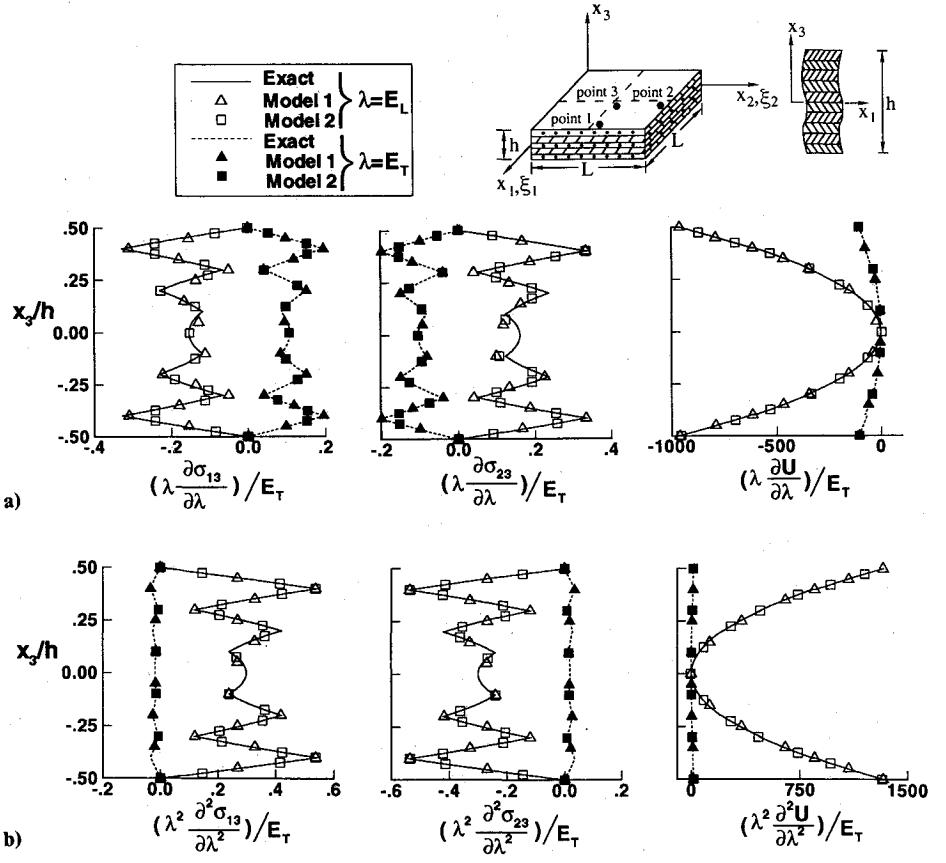


Fig. 9 Through-the-thickness distributions of first-order and second-order sensitivity coefficients of transverse shear stresses $\sigma_{13}$ at point 1, $\sigma_{23}$ at point 2, and strain energy density $U$ at point 3 obtained by exact three-dimensional thermoelasticity model; 10-layer cross-ply composite panel with $h/L = 0.05$, subjected to static loading $p = p_0 \sin \pi\xi_1 \sin \pi\xi_2$: a) first-order sensitivity coefficients and b) second-order sensitivity coefficients.

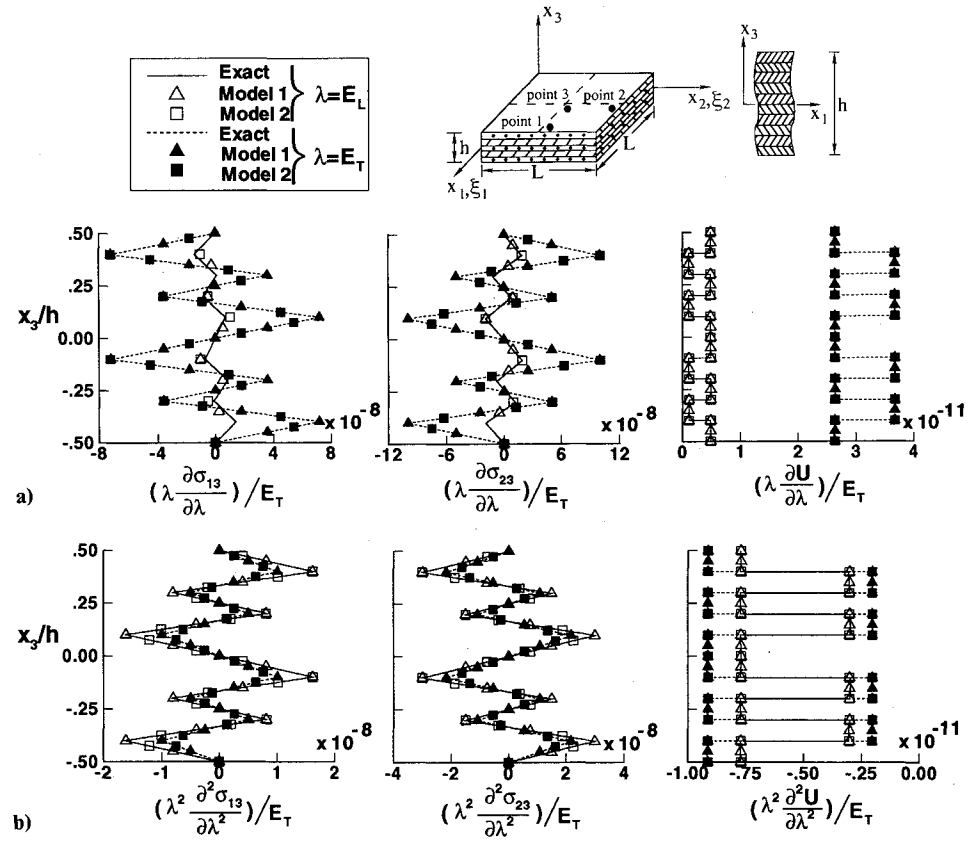


Fig. 10 Through-the-thickness distributions of first-order and second-order sensitivity coefficients of transverse shear stresses $\sigma_{13}$ at point 1, $\sigma_{23}$ at point 2, and strain energy density $U$ at point 3 obtained by exact three-dimensional thermoelasticity model; 10-layer cross-ply composite panel with $h/L = 0.05$, subjected to temperature change $T = T_0 \sin \pi\xi_1 \sin \pi\xi_2$: a) first-order sensitivity coefficients and b) second-order sensitivity coefficients.

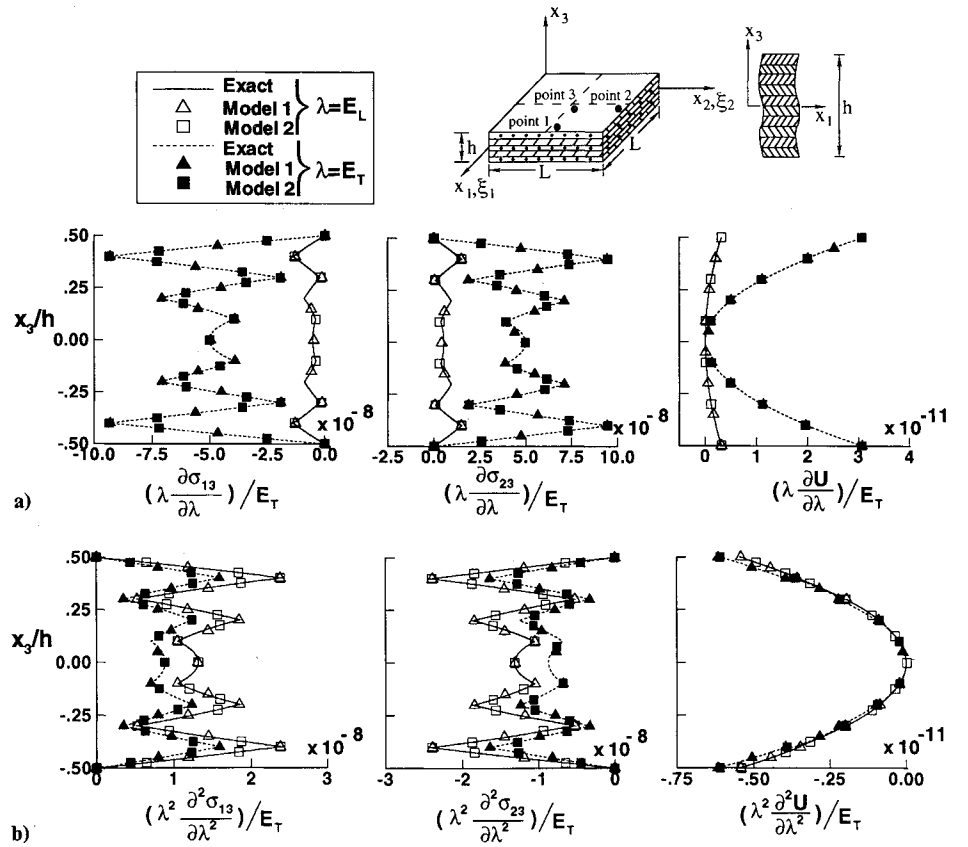


Fig. 11 Through-the-thickness distributions of first-order and second-order sensitivity coefficients of transverse shear stresses $\sigma_{13}$ at point 1, $\sigma_{23}$ at point 2, and strain energy density $U$ at point 3 obtained by exact three-dimensional thermoelasticity model; 10-layer cross-ply composite panel with $h/L = 0.05$, subjected to temperature gradient $T = x_3 T_1 \sin \pi\xi_1 \sin \pi\xi_2$: a) first-order sensitivity coefficients and b) second-order sensitivity coefficients.

the sensitivity coefficients. The results presented in these figures correspond to a $6 \times 6$ uniform grid in one quarter of the panel, with $\sigma_{13}$ evaluated at $\xi_1 = 0.958$, $\xi_2 = 0.542$ (point 1); $\sigma_{23}$ evaluated at $\xi_1 = 0.542$, $\xi_2 = 0.958$ (point 2); and $U$ evaluated at $\xi_1 = \xi_2 = 0.542$ (point 3).

An indication of the accuracy of the predictions of the 18-node three-dimensional finite element and the foregoing procedure, used in conjunction with the two-dimensional finite element and the degenerate solid element (models 1 and 2), is given in Figs. 2–5. An examination of Figs. 2–5 reveals the following:

1) For the $p_0$ and $T_1$ cases, $\sigma_{31}$ and $\sigma_{32}$ are symmetric with respect to the middle plane of the laminate. For the $T_0$ case, $\sigma_{13}$ and $\sigma_{23}$ are antisymmetric with respect to the middle plane. On the other hand, for all three cases $U$ is symmetric with respect to the middle plane.

2) The thickness distribution of the strain energy density predicted by the three-dimensional finite element model, with linear variation of the displacement components in the thickness direction, is fairly accurate, but the transverse shear stresses are only accurate at the center of each layer. This is true for each of the $p_0$, $T_0$, and $T_1$ cases considered (see Fig. 2). Several numerical experiments (results not shown here) have demonstrated that accurate determination of transverse shear stresses with three-dimensional finite elements requires using either more than one element in each layer or higher-order approximations for the displacements in the layer. Both approaches involve very high computational expense.

3) The foregoing computational procedure results in highly accurate thickness distributions for the transverse shear stresses and the total strain energy density for the $p_0$, $T_0$, and $T_1$ cases. This is particularly true for the thinner laminates with $h/L = 0.05$ (see Figs. 3, 4, and 5).

The thickness distributions of the normalized first-order and second-order sensitivity coefficients of the transverse shear stresses and total strain energy density, obtained by the exact solution of the three-dimensional thermoelasticity equations, are shown in Figs. 9–11 for the $p_0$, $T_0$, and $T_1$ cases, respectively. The sensitivity coefficients are each normalized through multiplying by $\lambda$ (or $\lambda^2$) and dividing by $E_T$.

For the $p_0$ case, the largest normalized first-order sensitivity coefficients for the transverse shear stresses and the total strain energy density are associated with $E_L$, $E_T$, and $G_{LT}$. However, the normalized second-order sensitivity coefficients associated with $E_L$ are considerably larger than those associated with $E_T$ and $G_{LT}$. For the $T_0$ and $T_1$ cases, the largest normalized first-order sensitivity coefficients are associated with $\alpha_T$ and $E_T$. However, the largest second-order sensitivity coefficients of the transverse shear stresses and total strain energy density are associated with ($E_L$, $E_T$), and $\alpha_T$, respectively.

An indication of the accuracy of the first-order and second-order sensitivity coefficients, with respect to $E_L$ and $E_T$, obtained by the foregoing computational procedure is given in Figs. 6–8, for the $p_0$, $T_0$, and $T_1$ cases, respectively. The high accuracy of the sensitivity coefficients predicted by the foregoing procedure is clearly demonstrated in these figures.

## V. Concluding Remarks

A computational procedure is presented for the accurate determination of the transverse shear stresses and their sensitivity coefficients in flat multilayered composite panels subjected to mechanical and thermal loads. The computational procedure can be used in conjunction with any two-dimensional or degenerate three-dimensional model. In the present study, two mixed finite element models are used for the spatial discretization of the panel. The first is a two-dimensional three-field model, based on a first-order shear deformation theory. The fundamental unknowns consist of the generalized displacements, the total strain components, and the stress resultants in the panel. The second model is a two-field degenerate solid element. The fundamental unknowns consist of the displacement components and the average mechanical strains through-the-thickness of the panel. Each of the displacement components is assumed to have a linear variation throughout the thickness of the laminate. The evaluation of the transverse shear stresses can be conveniently divided into two phases. The first phase consists of using a superconvergent recovery technique for evaluating the in-plane stresses in the different layers. In the second phase, the thickness distributions of the transverse shear stresses are evaluated by using piecewise integration, in the thickness direction, of the three-dimensional equilibrium equations. The same procedure is used for evaluating the sensitivity coefficients of the transverse shear stresses (first-order and second-order derivatives of transverse shear stresses with respect to lamination and material parameters).

The effectiveness of the computational procedure is demonstrated by means of numerical examples of multilayered cross-ply panels subjected to transverse loading, uniform temperature change, and uniform temperature gradient through the thickness of the panel. In each case, the predictions of the foregoing procedure were compared with those of three-dimensional finite element models, as well as with exact solution of the three-dimensional thermoelasticity equations of the panel. For panels with $h/L \leq 0.1$, the response and sensitivity coefficients predicted by the foregoing procedure are highly accurate. The errors in the predictions of the foregoing procedure are expected to increase with the increase in the thickness ratio of the panel. For thick panels with $h/L \geq 0.2$, accurate determination of transverse stresses and sensitivity coefficients may require the use of the predictor-corrector approaches, such as the ones described in Refs. 16 and 17. The foregoing procedure can be easily extended to curved shell structures.

## Appendix A: Thermoelastic Constitutive Relations for the Laminate

The linear thermoelastic two-dimensional finite element model (model 1) used in the present study is based on the following assumptions:

1) The laminates are composed of a number of perfectly bonded layers.

2) Every point of the laminate is assumed to possess a single plane of thermoelastic symmetry parallel to the middle plane.

3) The material properties are independent of temperature.

4) The constitutive relations are described by a first-order shear-deformation type lamination theory, and can be written in the following compact form:

$$\begin{Bmatrix} \boldsymbol{N} \\ \boldsymbol{M} \\ \boldsymbol{Q} \end{Bmatrix} = \begin{bmatrix} [\boldsymbol{A}] & [\boldsymbol{B}] & 0 \\ [\boldsymbol{B}]^t & [\boldsymbol{D}] & 0 \\ 0 & 0 & [\boldsymbol{A}_s] \end{bmatrix} \begin{Bmatrix} \varepsilon \\ \kappa \\ \gamma \end{Bmatrix} - \begin{Bmatrix} \boldsymbol{N}_T \\ \boldsymbol{M}_T \\ 0 \end{Bmatrix} \tag{A1}$$

where $\{\boldsymbol{N}\}$, $\{\boldsymbol{M}\}$, $\{\boldsymbol{Q}\}$, $\{\varepsilon\}$, $\{\kappa\}$, and $\{\gamma\}$ are given by

$$\{\boldsymbol{N}\}^t = \left[N_1 \; N_2 \; N_{12}\right] \tag{A2}$$

$$\{\boldsymbol{M}\}^t = \left[M_1 \; M_2 \; M_{12}\right] \tag{A3}$$

$$\{\boldsymbol{Q}\}^t = \left[Q_1 \; Q_2\right] \tag{A4}$$

$$\{\varepsilon\}^t = \left[\varepsilon_1^0 \; \varepsilon_2^0 \; 2\varepsilon_{12}^0\right] \tag{A5}$$

$$\{\kappa\}^t = \left[\kappa_1^0 \; \kappa_2^0 \; 2\kappa_{12}^0\right] \tag{A6}$$

$$\{\gamma\}^t = \left[2\varepsilon_{31} \; 2\varepsilon_{32}\right] \tag{A7}$$

The matrices $[A]$, $[B]$, $[D]$, and $[A_s]$ can be expressed in terms of the layer stiffnesses as follows:

$$\left[[A]\ \ [B]\ \ [D]\right] = \sum_{k=1}^{NL} \int_{h_{k-1}}^{h_k} [\bar{Q}]^{(k)} \left[[I]\ \ x_3[I]\ \ (x_3)^2[I]\right] dx_3 \tag{A8}$$

$$[A_s] = \sum_{k=1}^{NL} \int_{h_{k-1}}^{h_k} [\bar{Q}_s]^{(k)}\, dx_3 \tag{A9}$$

where $[I]$ is the identity matrix. The expressions for the different coefficients of the matrices $[\bar{Q}]^{(k)}$ and $[\bar{Q}_s]^{(k)}$ in terms of the material and geometric properties of the constituents (fiber and matrix) are given in Refs. 18 and 19.

The vectors of thermal forces and moments, $\{N_T\}$ and $\{M_T\}$, are given by

$$\left[\{N_T\}\ \ \{M_T\}\right] = \sum_{k=1}^{NL} \int_{h_{k-1}}^{h_k} [\bar{Q}]^{(k)} \{\alpha\}^{(k)} \left[1\ \ x_3\right] T\, dx_3 \tag{A10}$$

See, for example, Refs. 20 and 21.

## Appendix B: Form of the Arrays in the Governing Finite Element Equations of the Panel

The form of the arrays in the governing finite element equations, Eqs. (1), for the two models used in the present study are given in this Appendix. In Table B1, 0 refers to a null matrix or a null vector.

## Appendix C: Explicit Form of the Array $[K]$, $[R]$, $\{H_T\}$; $[\bar{K}]$, $[S_1]^t$, and $\{\bar{H}_T\}$

For model 1, two sets of Lagrangian shape functions are used: biquadratic shape functions to approximate each of the generalized displacement components, and bilinear shape functions to approximate each of the total strain components, and stress resultants. For model 2, the same set of biquadratic shape functions is used for approximating each of the generalized displacement components in the $x_1 - x_2$ plane as in model 1. However, different sets of shape functions are used for approximating the different components of the average mechanical strains through the thickness (average in-plane extensional strains, the two transverse shear strains, and the transverse normal strain; see Ref. 13). For model 2, the approximations for the average mechanical strain and total strain vectors within an element can be expressed in terms of the strain and displacement parameters, as follows:

**Table B1**

| Array | Model 1—three-field model | Model 2—two-field model |
|---|---|---|
| $\{Z\}$ | $\begin{Bmatrix} E \\ H \\ X \end{Bmatrix}$ | $\begin{Bmatrix} \bar{E} \\ X \end{Bmatrix}$ |
| $[K]$ | $\begin{bmatrix} [K] & [R] & [0] \\ [R]^t & [0] & [S] \\ [0] & [S]^t & [0] \end{bmatrix}$ | $\begin{bmatrix} [\bar{K}] & [S_1] \\ [S_1]^t & [0] \end{bmatrix}$ |
| $\{Q^{(1)}\}$ | $\begin{Bmatrix} 0 \\ 0 \\ P \end{Bmatrix}$ | $\begin{Bmatrix} 0 \\ P \end{Bmatrix}$ |
| $\{Q^{(2)}\}$ | $\begin{Bmatrix} H_T \\ 0 \\ 0 \end{Bmatrix}$ | $\begin{Bmatrix} \bar{H}_T \\ 0 \end{Bmatrix}$ |

$$\{\bar{\varepsilon}\}^{(e)}_{\text{mech}} = [R_1]^{(e)} \{\bar{E}\}^{(e)} \tag{C1}$$

$$\{\bar{\varepsilon}\}^{(e)}_{\text{tot}} = [\bar{B}]^{(e)} \{X\}^{(e)} \tag{C2}$$

where superscript $(e)$ refers to individual elements. Note that the actual mechanical strain components can be discontinuous at the layer interfaces. The expression of the actual mechanical strain vector in the $k$th layer of an element can be written in the following form:

$$\{\varepsilon\}^{(e)}_{\text{mech}} = -\left([R_1][\bar{K}]^{-1}[S_1]\{X\}\right)^{(e)} - \left(\{\alpha\}^{(k)} T\right)^{(e)} \tag{C3}$$

It is convenient to partition the arrays (matrices and vectors), for individual elements, into blocks and subvectors. The expressions for the typical blocks $(i', j')$ and $(i', j)$ of the arrays, and the typical partitions $i'$ of the vectors for models 1 and 2 are given subsequently:

Model 1:

$$[K]_{i',j'} = \int_{\Omega^{(e)}} \begin{bmatrix} [A] & [B] & 0 \\ [B]^t & [D] & 0 \\ 0 & 0 & [A_s] \end{bmatrix} \bar{N}_{i'} \bar{N}_{j'}\, d\Omega \tag{C4}$$

$$[R]_{i',j'} = \int_{\Omega^{(e)}} [I] \bar{N}_{i'} \bar{N}_{j'}\, d\Omega \tag{C5}$$

$$\{H_T\}_{i'} = \int_{\Omega^{(e)}} \begin{Bmatrix} N_T \\ M_T \\ 0 \end{Bmatrix} \bar{N}_{i'}\, d\Omega \tag{C6}$$

Model 2:

$$[\bar{K}]_{i',j'} = \int_{\Omega^{(e)}} [R_1]^t_{i'} [C] [R_1]_{j'}\, d\Omega \tag{C7}$$

$$[S_1]_{i',j} = \int_{\Omega^{(e)}} [R_1]^t_{i'} [C] [\bar{B}]_j\, d\Omega \tag{C8}$$

$$\{\bar{H}_T\}_{i'} = \int_{\Omega^{(e)}} [R_1]^t_{i'} \left( \sum_{k=1}^{NL} \int_{h_{k-1}}^{h_k} [\bar{C}]^{(k)} \{\alpha\}^{(k)} T\, dx_3 \right) d\Omega \tag{C9}$$

In Eqs. (C7) and (C9), $[C]$ is the $6 \times 6$ effective stiffness matrix of the laminate, given by

$$[C] = \sum_{k=1}^{NL} \int_{h_{k-1}}^{h_k} [\bar{C}]^{(k)}\, dx_3 \tag{C10}$$

where $[\bar{C}]^{(k)}$ is the $6 \times 6$ reduced material stiffness matrix of the $k$th layer (based on neglecting the coupling between the transverse normal strain and the extensional strain components; see Ref. 13).

In Eqs. (C6–C9), the subscripts $i'$ (or $j'$) and $j$ refer to the partitions of the matrices $[R_1]$ and $[\bar{B}]$ associated with the $i'$ (or $j'$) and the $j$th shape function used in approximating the average mechanical strains and generalized displacements, respectively. Note that in model 2 the transverse normal strain and transverse normal stresses are included.

## Appendix D: Determination of the Thickness Distributions of the Transverse Shear Stresses and the Total Strain Energy Density

The procedure used for calculating the thickness distribution of the transverse shear stresses $\sigma_{3\beta}$ and the strain energy density $U$, is as follows:

1) For model 1 the middle surface strains $\varepsilon^0_{\beta\gamma}$ and curvature changes $\kappa^0_{\beta\gamma}$ are calculated at the numerical quadrature points of each finite element using the total strain vector $\{E\}$ for individual elements and the bilinear shape functions. Then the in-plane stresses in each layer $\sigma_{\alpha\beta}$ are calculated using the following relations (for a typical layer $k$)[18,19]:

$$\sigma^{(k)}_{\beta\gamma} = \bar{c}^{(k)}_{\beta\gamma\rho\delta}[\varepsilon^0_{\rho\delta} + x_3\kappa^0_{\rho\delta} - \alpha_{\rho\delta}T^{(k)}] \tag{D1}$$

where a repeated subscript in the same term denotes summation over its entire range 1, 2.

For model 2, the in-plane stresses are calculated using the actual mechanical strain components [Eqs. (C3)] and the following relation:

$$\sigma^{(k)}_{\beta\gamma} = \bar{c}^{(k)}_{\beta\gamma\rho\delta}\varepsilon_{\rho\delta} \tag{D2}$$

2) The transverse shear stresses in each layer are obtained by integrating the three-dimensional equilibrium equations in the thickness direction as follows:

$$\sigma_{3\beta} = -\int_{-h/2}^{x_3} \partial_\gamma \sigma_{\gamma\beta}\, dx_3 + c_\beta \tag{D3}$$

where $c_\beta$ are integration constants obtained from the stress conditions at the top and bottom surfaces of the laminate, and $\partial_\gamma \equiv (\partial/\partial x_\gamma)$. Because of the discontinuity of $\sigma_{\gamma\beta}$ at layer interfaces, the integrations of Eqs. (D3) are performed in a piecewise manner (layer-by-layer).

3) The transverse shear strains are obtained by using the three-dimensional constitutive relations, as follows[18]:

$$2\varepsilon_{3\beta} = a_{3\beta3\gamma}\sigma_{3\gamma} \tag{D4}$$

4) The strain energy density $U$ is obtained by using the following expression:

$$U = 1/2\,\sigma_{\beta\gamma}(\varepsilon^0_{\beta\gamma} + x_3\kappa^0_{\beta\gamma} - \alpha_{\beta\gamma}T) + 2\sigma_{3\beta}\varepsilon_{3\beta} \tag{D5}$$

In model 2, the contribution of $(\sigma_{33}, \varepsilon_{33})$ to $U$ is neglected.

5) The transverse shear stresses $\sigma_{3\beta}$, and the strain energy density $U$ are then interpolated from the numerical quadrature points to the center of the finite element.

## Acknowledgments

The present research is supported by a NASA Cooperative Agreement NCCW-0011 and by an Air Force Office of Scientific Research Grant AFOSR-F49620-93-1-0184. The authors appreciate the useful discussions with and the encouragement from the grant monitors, Samuel L. Venneri, of NASA Headquarters, and C. I. Chang and W. F. Jones of AFOSR.

## References

[1]Mau, S. T., Tong, P., and Pian, T. H. H., "Finite Element Solution for Laminated Thick Plates," *Journal of Composite Materials*, Vol. 6, April 1972, pp. 304–311.

[2]Spilker, R. L., Chou, S. C., and Orringer, O., "Alternate Hybrid-Stress Elements for Analysis of Multilayer Composite Plates," *Journal of Composite Materials*, Vol. 11, Jan. 1977, pp. 51–70.

[3]Spilker, R. L., "Hybrid-Stress Eight-Node Elements for Thin and Thick Multilayer Laminated Plates," *International Journal for Numerical Methods in Engineering*, Vol. 18, No. 6, 1982, pp. 801–828.

[4]Owen, D. R. J., and Li, Z. H., "A Refined Analysis of Laminated Plates by Finite Element Displacement Method—1: Fundamentals and Static Analysis," *Computers and Structures*, Vol. 26, No. 6, 1987, pp. 907–914.

[5]Robbins, D. H., Jr., and Reddy, J. N., "Modeling of Thick Composites Using a Layerwise Laminate Theory," *International Journal for Numerical Methods in Engineering*, Vol. 36, No. 4, 1993, pp. 655–677.

[6]Pryor, C. W., Jr., and Barker, R. M., "A Finite Element Analysis Including Transverse Shear Effects for Application to Laminated Plates," *AIAA Journal*, Vol. 9, No. 5, 1971, pp. 912–917.

[7]Govindarajan, R., Krishna Murty, A. V., Vijayakumar, K., and Raghuram, P. V., "Finite Element Estimation of Elastic Interlaminar Stresses in Laminates," *Composites Engineering*, Vol. 3, No. 5, 1993, pp. 451–466.

[8]Chaudhuri, R. A., and Seide, P., "An Approximate Semi-Analytical Method for Prediction of Interlaminar Shear Stresses in an Arbitrary Laminated Thick Plate," *Computers and Structures*, Vol. 25, No. 4, 1987, pp. 627–636.

[9]Reddy, J. N., Barbero, E. J., and Teply, J. L., "A Plate Bending Element Based on a Generalized Laminate Plate Theory," *International Journal for Numerical Methods in Engineering*, Vol. 28, No. 10, 1989, pp. 2275–2292.

[10]Chaudhuri, R. A., "An Equilibrium Method for Reduction of Transverse Shear Stresses in a Thick Laminate Plate," *Computers and Structures*, Vol. 23, No. 2, 1986, pp. 139–146.

[11]Engblom, J. J., and Ochoa, O. O., "Through the Thickness Stress Predictions for Laminated Plates of Advanced Composite Materials," *International Journal for Numerical Methods in Engineering*, Vol. 21, No. 10, 1985, pp. 1759–1776.

[12]Kant, T., and Pandya, B. N., "A Simple Finite Element Formulation of a Higher-Order Theory for Unsymmetrically Laminated Composite Plates," *Composite Structures*, Vol. 9, No. 3, 1988, pp. 215–246.

[13]Kim, Y. H., and Lee, S. W., "A Solid Element Formulation for Large Deflection Analysis of Composite Shell Structures," *Computers and Structures*, Vol. 30, No. 1/2, 1988, pp. 269–274.

[14]Srinivas, S., and Rao, A. K., "Bending, Vibration and Buckling of Simply-Supported Thick Orthotropic Rectangular Plates and Laminates," *International Journal of Solids and Structures*, Vol. 6, 1970, pp. 1464–1481.

[15]Pagano, N. J., "Exact Solutions for Rectangular Bidirectional Composites and Sandwich Plates," *Journal of Composite Materials*, Vol. 4, Jan. 1970, pp. 20–34.

[16]Noor, A. K., Burton, W. S., and Peters, J. M., "Predictor-Corrector Procedure for Stress and Free Vibration Analyses of Multilayered Composite Plates and Shells," *Computer Methods in Applied Mechanics and Engineering*, Vol. 82, Nos. 1–3, 1990, pp. 341–364.

[17]Noor, A. K., and Burton, W. S., "Accuracy of Critical-Temperature Sensitivity Coefficients Predicted by Multilayered Composite Plate Theories," *AIAA Journal*, Vol. 30, No. 9, 1992, pp. 2283–2290.

[18]Jones, R. M., *Mechanics of Composite Materials*, McGraw-Hill, New York, 1975.

[19]Tsai, S. W., and Hahn, H. T., *Introduction to Composite Materials*, Technomic Publishing, Westport, CT, 1980.

[20]Padovan, J., "Anisotropic Thermal Stress Analysis," *Thermal Stresses I*, edited by R. B. Hetnarski, Elsevier, Amsterdam, The Netherlands, 1986, pp. 143–262.

[21]Bert, C. W., "Analysis of Plates," *Composite Materials*, edited by C. C. Chamis, Vol. 7, Structural Design and Analysis, Part I, Academic, New York, 1975, pp. 149–206.